

S2FGAN: Semantically Aware Interactive Sketch-to-Face Translation

Yan Yang¹ Md Zakir Hossain¹ Tom Gedeon¹ Shafin Rahman²

¹The Australian National University ²North South University

{u6169130, zakir.hossain, tom.gedeon}@anu.edu.au, shafin.rahman@northsouth.edu

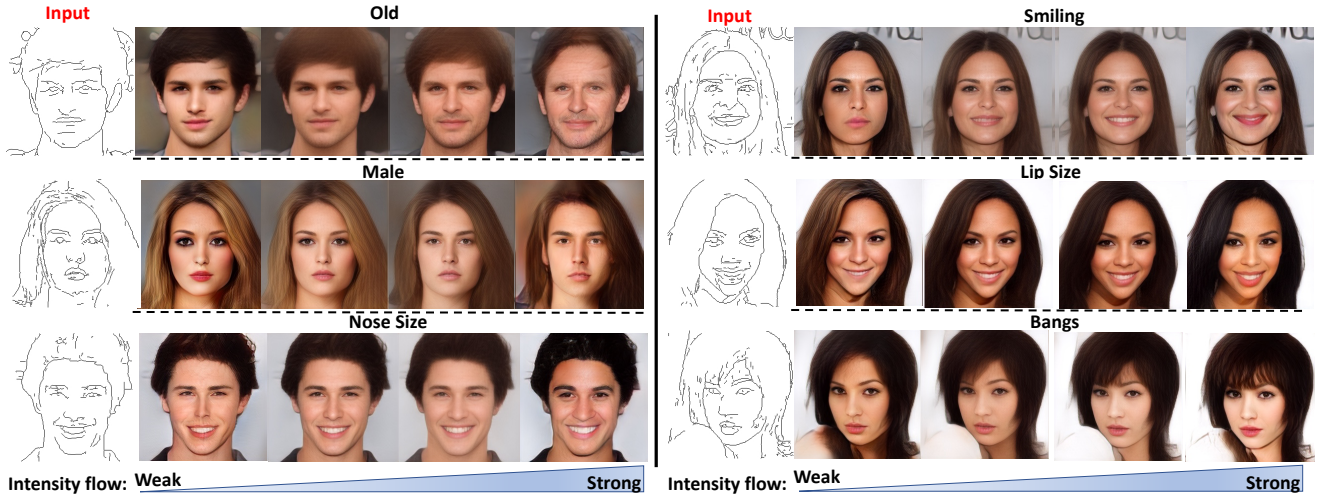


Figure 1: Our proposed **S2FGAN** framework generates the photo-realistic face from a face sketch image as **input** and manipulates single or multiple attributes (age, gender, nose, smiles, lips, bangs, and so on) of faces with greater control.

Abstract

Interactive facial image manipulation attempts to edit single and multiple face attributes using a photo-realistic face and/or semantic mask as input. In the absence of the photo-realistic image (only sketch/mask available), previous methods only retrieve the original face but ignore the potential of aiding model controllability and diversity in the translation process. This paper proposes a sketch-to-image generation framework called **S2FGAN**, aiming to improve users’ ability to interpret and flexibility of face attribute editing from a simple sketch. The proposed framework modifies the constrained latent space semantics trained on Generative Adversarial Networks (GANs). We employ two latent spaces to control the face appearance and adjust the desired attributes of the generated face. Instead of constraining the translation process by using a reference image, the users can command the model to retouch the generated images by involving the semantic information in the generation process. In this way, our method can manipulate single or multiple face attributes by only specifying attributes to be changed. Extensive experimental results on CelebAMask-HQ dataset empirically shows our superior performance and effectiveness on this task. Our method successfully outperforms state-of-the-art methods on attribute manipulation by exploiting greater control of attribute intensity.

1. Introduction

Generative Adversarial Networks (GANs) [4] is one of the emerging techniques for image synthesis and achieves tremendous success in image-to-image (I2I) translation. Now, generating photo-realistic faces from sketches becomes possible by learning pixel-wise correspondence using conditional GANs [20, 18, 30, 28, 7]. Although such techniques remain successful in enabling a novice artist to restore a face from a sketch, they often fail to control specific facial attributes’ intensity. For example, a user may wish to add a specific attribute, such as a smile, after generating a face from a drawing and/or s/he may wish to control intensities of facial attributes. For non-artists, modifying the sketches is very hard for describing facial features such as happiness, age, or chubby. However, it is easy to specify those abstract appearances (attribute/semantic) as text input. This paper investigates how a GAN model can increase such users’ interpretability and flexibility of attributes editing from a simple sketch.

We identify several limitations in this line of investigation. (a) Existing methods perform attribute editing when the input is a photo-realistic face [2, 5, 17, 14, 25]. These methods cannot work in the absence of a photo-realistic image as input. (b) Although methods can successfully add or remove attributes (like age, gender, beard) from photo-

realistic faces, they are not able to provide adequate measures to control intensities of attributes. Recent approaches have somewhat addressed this issue, but they mostly fail to preserve subjects identify at higher intensity boundary of attributes. Moreover, many methods ignore state-like attributes, such as *chubby*, which are expected to have diverse intensities. [2, 17, 5, 14, 25] (c) For attribute editing, users need to specify both the attributes intended to be preserved and changed, increasing the necessity of manual annotations [5, 14, 2]. Recent approaches, InterFaceGAN [25] and STGAN [17] allow users to edit face attributes by specifying attributes to be changed only. However, none of those methods can work when the input is a sketch.

This paper presents a novel sketch-to-face GAN framework, *S2FGAN*, to aid the controllability of image attributes in sketch-to-image generation. We notice that a large dimensionality latent space usually preserves the input identity, but causes the difficulty for latent space manipulations in image-to-image translation [11]. Instead, a low dimensionality latent space gives the reverse behaviors. Here, we propose using two latent spaces: an appearance latent space with large dimensionality for identity preservation and another latent space with low dimensionality for attribute editing. Our network projects the given input sketch to both appearance and attribute editing latent spaces. Then, this network mixes the attribute shifting vector with the attribute editing latent code based on cosine similarity. This mixer affects the convolution weights which were used for decoding the appearance latent code. Specifically, different inputs have different convolution weights for decoding. The network learns to activate different convolution filters based on desired attribute shifts. In this way, we preserve identity and edit multiple attributes simultaneously based on only specifying attributes to be changed, and manipulate the attribute intensity with greater control. Figure 1 shows some sample outputs of our method. Comparing with the state-of-the-art methods in Figure 5, our model provides smooth attributes intensity control. Furthermore, we achieve superior attribute editing and diversity control performance, especially when manipulating multiple attributes, as shown in Figure 4.

Overall, our contributions are summarised below:

- We propose the *S2FGAN* framework for sketch-to-image translation with the facility of face reconstruction, attribute editing, and interactive manipulation of attribute intensity. Our model can work on both single and multiple attribute editing and manipulation problems. Further, users can control intensities of attributes by only specifying/changing target attributes (semantics) and preserving face identity.
- Unlike previous approaches, our framework uses two latent spaces called appearance and attribute editing la-

tent spaces separately. By maintaining the appropriate dimension of latent spaces, we calibrate face attributes with broader control, diversity, and smoothness.

- We present extensive experiments by comparing with state-of-the-art methods (AttGAN [5], STGAN [17]) and alternative baselines. We achieve superior performance on attribute editing and intensity control in our target sketch-to-image translation task, especially when multiple attributes are involved in the process.

2. Related Work

Face-to-Face translation. Generative Adversarial Networks (GANs) have shown great potential in computer vision tasks such as high-resolution image synthesis [10, 11, 12, 28], image completion [8, 30, 22], image translation [18, 30, 22, 25, 7, 2, 5, 14, 16, 6], and conditional image synthesis [20, 18, 8, 22]. Among these applications, face-to-face translation is one of the most widely studied tasks, because faces carry influential social cues essential for human communication. There are two streams of studies in this domain. The first stream focuses on a mask- or sketch-to-face translation. A representative model of this kind, Pix2Pix [7] receives training with paired faces in a supervised manner by minimizing L1 and adversarial loss, and is capable of generating photo-realistic face samples. Here, models have limited control over face attributes because of the lack of expressiveness of specific facial features. The second stream focuses on the latent space of GANs to achieve smooth interpolation from one face-feature to another face-feature [13, 1, 24, 27, 25]. Here, models encode a face to a low-dimensional vector and decode the vector to generate the desired output. One of the most significant challenges in this stream is GAN inversion, which aims to decode the input image to the latent space vector. A recent work, ALD [21], tries to address this problem, but preservation of face identity remains questionable. Our proposed approach follows the second stream, but instead of a single latent space, we encode the input into two latent spaces. One latent space preserves subject identity information, and the other provides the flexibility of desired latent space manipulation.

Attribute Editing. In Face-to-Face translation, attribute editing attempts to change certain features (e.g., big lips/big smile) of a given face with the condition of preserving identity information. Some methods edit attributes of photo-realistic images by using pencil sketch as input [8, 30]. Others edit the image attributes by keyword descriptions (e.g., Male and Young) [2, 5, 14, 17]. Because it requires less manual interaction, this paper explores the latter approach. A known issue about keyword-based editing is that it requires manually specifying both attributes to be edited and preserved [5, 2, 14]. In recent works, STGAN [17] addressed this issue by improving the generation process

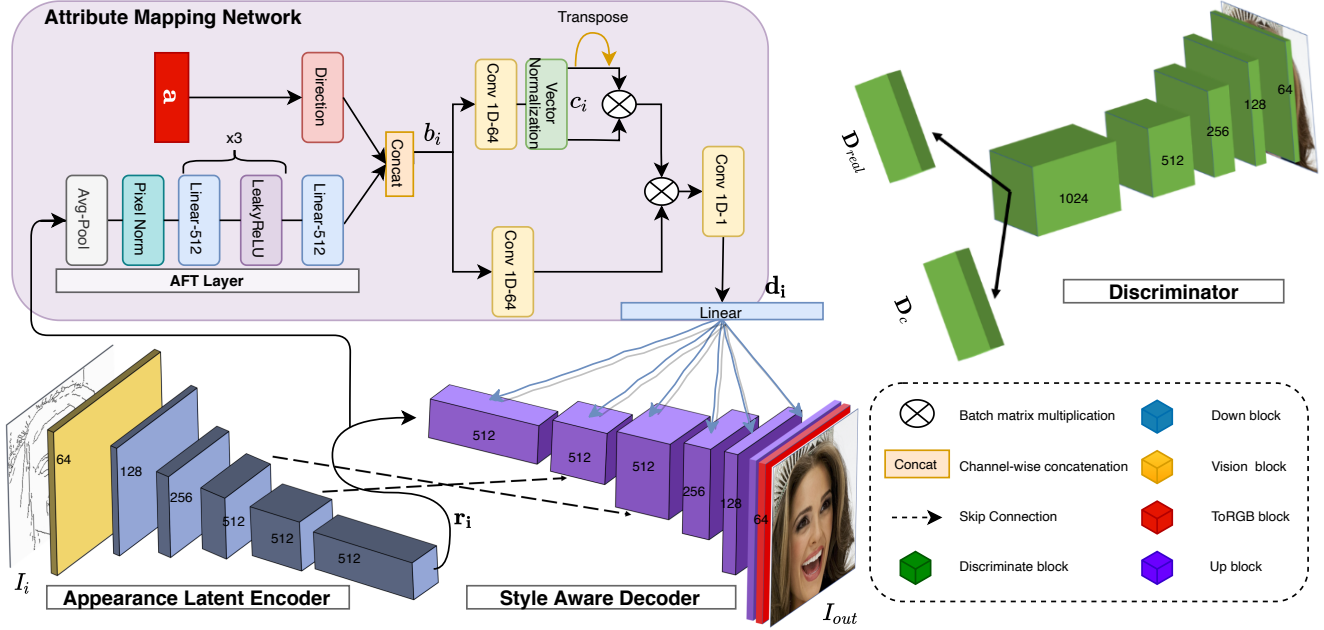


Figure 2: The network architecture of *S2FGAN* framework. The input face I_i is projected to appearance latent code \mathbf{r}_i via Appearance Latent Encoder and to attribute editing code \mathbf{d}_i via Attribute Mapping Networks based on interactive semantic guidance from \mathbf{a} . And, \mathbf{r}_i contains the face identity information, and \mathbf{d}_i helps the Style Aware Decoder to create desired convolution filters for manipulated face I_{out} . The discriminator structure provides necessary supervision to support the generator.

of AttGAN [5]. However, they did not consider assisting the generation process of diverse image-to-image translation problems by involving semantic attributes. Another recent work, InterfaceGAN [25], successfully included a control on diverse image generation by editing the latent code proposed in StyleGAN [11] or PGGAN [10]. This approach could lead to messy results when the attributes pool is large (more than three). Moreover, to get photo-realistic results, methods randomly sample a latent code instead of encoding an image to the latent code and then manipulate the attribute semantics. All existing works of attribute editing operate on the domain of photo-realistic images, which lacks generalization ability. This paper focuses on attribute editing in the absence of photo-realistic images (e.g., uses a sketch or edges) that can help users express their abstract ideas by compensating for the limited representation power of sketches, masks, and so on.

Sketch-to-Image Generation. This enables non-artists to simulate diverse images by sketching their abstract ideas. The goal is to map the sketch to their corresponding ground truth images [30, 18, 28, 7, 3]. Previous work such as Deep Plastic Surgery [30] and ContextualGAN [18] had a target of increasing the model robustness by adapting poorly drawn sketches. However, they did not consider improving the generation process by including semantic descriptions from users. As a result, they could not control the diversity of image attributes. This paper aims to help the sketch-to-

image generation processes by providing the opportunities to control intensities of attributes.

3. Method

Problem Formulation. Suppose, \mathbf{A} represents the set of valid attributes (i.e. smile, old and so on) of faces. Given a sketch image $I_i \in \mathbb{R}^{H \times W}$ and desired attributes shifting vector $\mathbf{a} = [a_1, a_2 \dots a_{|\mathbf{A}|}] \in \mathbb{R}^{|\mathbf{A}|}$, our goal is to find a parameterized generator \mathbf{G} that learns a mapping, $\mathbf{G}(I_i, \mathbf{a}) \rightarrow I_{out}$ from the sketch, I_i to photo-realistic image, $I_{out} \in \mathbb{R}^{H \times W \times 3}$ described by the attributes shifting vector \mathbf{a} . By manipulating \mathbf{a} , users can control intensity of attributes in a generated face I_{out} . When $\mathbf{a} = \mathbf{0} \in \mathbb{R}^{|\mathbf{A}|}$, $\mathbf{G}(I_i, \mathbf{0})$ reconstructs the ground truth photo-realistic image, I_{gt} appeared in the sketch only. Otherwise, $\mathbf{G}(I_i, \mathbf{a})$ generates manipulated photo-realistic face according to the value of \mathbf{a} . Shifting the value $a_j \in [0, 1]$ manipulates the j th attribute of face. Users have the flexibility to manipulate both single or multiple attributes a_j where $j = 1, 2 \dots |\mathbf{A}|$ simultaneously.

3.1. S2FGAN Framework

We introduce our proposed framework, *S2FGAN*, in Figure 2. It has two key components: a Generator (Appearance Latent Encoder, Attribute Mapping Network, and Style Aware Decoder) and a Discriminator. The Appearance Latent Encoder aims to learn critical appearance in-

formation of input. Attribute Mapping Networks manipulate the latent space to create/remove desired attributes by collaborating with a Style Aware Decoder, that scales the convolution’s weight.

Appearance Latent Encoder. The vision block, down blocks consist of our Appearance Latent Encoder, which is convolution-based down sampling. The Appearance Latent Encoder takes I_i as input and produces \mathbf{r}_i as output.

Attribute Mapping Network. This sub-network takes the output of Appearance Latent Encoder \mathbf{r}_i of the Appearance Latent Encoder and the attribute shifting vector \mathbf{a} as inputs. The \mathbf{r}_i is further processed by Appearance Feature Transform (AFT) that is composed of a down block, a global average pooling layer, a pixel normalization layer [11], and a multi-layer perceptron. There is an embedding layer named direction that maintains $|\mathbf{A}|$ trainable vectors, which compose a matrix \mathbf{S} . Each vector represents a unit of semantic for each attribute. This layer takes attribute shifting vector as input \mathbf{a} , and perform the element-wise multiplication with the semantic matrix \mathbf{S} . We project the output of the direction layer and AFT layer onto the latent space. Here, we manipulate the attributes of I_{out} by using vector normalization, matrix multiplication, and convolution1D layers interchangeably. Let f_1, f_2 , and f_3 denote three convolution 1D layers respectively.

$$\mathbf{b}_i = \text{concat}(AFT(\mathbf{r}_i), \mathbf{a} \times \mathbf{S}) \quad (1)$$

$$\mathbf{c}_i = \mathbf{N}(f_1(\mathbf{b}_i)) \quad (2)$$

$$\mathbf{d}_i = f_3(\mathbf{c}_i \otimes \mathbf{T}(\mathbf{c}_i) \otimes f_2(\mathbf{b}_i)) \quad (3)$$

concat , \mathbf{N} , \mathbf{T} , \times , and \otimes represent channel-wise concatenation, vector normalization along channel dimension, transpose channel dimension with the last dimension, element-wise multiplication, and batch matrix multiplication, respectively. \mathbf{b}_i and \mathbf{c}_i are intermediate variables. We forward \mathbf{d}_i to the up block for decoding the image from appearance latent space. First, we process \mathbf{b}_i by a convolution 1D layer f_1 , then (vector) normalize each attribute semantic (including the processed appearance latent codes) for self-matrix multiplication. $\mathbf{c}_i \otimes \mathbf{T}(\mathbf{c}_i) \in \mathbb{R}^{(|A|+1) \times (|A|+1)}$ contains the cosine similarity between each individual latent code pair (which is separated on channel dimension). Second, we encapsulate a unified attribute editing latent code by using f_3, f_2 , and matrix multiplication. This latent code should be changed with the awareness of how the rest of them are similar to each other. Note that the output channel of f_3 is fixed to 1. To weakly guide the learning process, instead of explicitly defining how the attribute editing latent code should be shifted, we use conv. 1D layers with an input of cosine similarity for attribute semantics. Unlike the linear assumption on latent space from InterFaceGAN [25], here, we do not rely on the latent space linearity. This idea is especially helpful when multiple attributes editing is involved in a latent space. In this way, we can adapt to

arbitrary complex attribute editing while preserving the appearance of the sketch I_i .

Style Aware Decoder. Our up block uses the Style Block of StyleGAN as backbone [12]. According to StyleGAN [11], the size of feature maps determines the subset of attributes that can be appropriately edited. To persist the appearance of input I_i , we adopt U-NET-like [23] skip connections from feature map size 4×4 to 16×16 . After an affine transformation (one linear layer) of \mathbf{d}_i , it is used to scale the weights of the modulated convolution layer and modify attributes in the appearance latent space defined below.

$$w'_{jkl} = q_j \times w_{jkl} \quad (4)$$

w and w' represent original weights and scaled weights, respectively. q_j is the corresponding scale for j_{th} channel of weight matrix after applying the affine transformation to \mathbf{d}_i . The modulated convolution layer scales its weights by its standard deviation as follows:

$$w''_{jkl} = \frac{w'_{jkl}}{\sqrt{\sum_{j,l} w'_{jkl}{}^2 + \epsilon}} \quad (5)$$

w''_{jkl} is scaled weights used for the convolution operation. When concatenating the down-sampled input with labels to generate attributed outputs similar to [5, 2, 17, 14], the networks can learn to eliminate the conflicting features and create the desired characteristics. However, it also increases the complexity of the problem. Instead of directly scaling the weights of the convolution layer, our network learns to activate different filters given the desired attributes.

Discriminator Structure. Following recent works [2, 8, 7], we adapt the PatchGAN to serve as the discriminator of our framework. The discriminator aims to distinguish the real and fake samples and classify the attributes of samples. The outputs of discriminator \mathbf{D}_{real} and \mathbf{D}_c represent the score of belonging to the photo-realistic and class domain, respectively.

3.2. Multi-Objective Learning

There are five objective functions in our framework. Let \mathcal{S} denote softplus activation function. We denote I_{gt} as the ground truth photo-realistic images for sketch I_i , while u_i are the attributes of ground truth images.

Adversarial Loss. We use adversarial loss, \mathcal{L}_{adv}^r to encourage the generated sample from generator \mathbf{G} to be indistinguishable for the discriminator. This is a non-saturating logistic loss [4], defined as follows:

$$\mathcal{L}_{adv}^r = \mathbb{E}[\mathcal{S}(-\mathbf{D}_{real}(\mathbf{G}(I_i, \mathbf{a})))] \quad (6)$$

The discriminator \mathbf{D} tries to distinguish the generated samples from real samples by minimizing \mathcal{L}_{adv}^l .

Table 1: Attribute statistic of CelebAMask-HQ. The value indicates the number of times each attribute appeared in faces.

Attribute Fold	Smiling	Male	No_Beard	Eyeglasses	Young	Bangs	Narrow_Eyes	Pale_Skin	Big_Lips	Big_Nose	Mustache	Chubby
Training	13446	10512	23084	1404	22194	5141	3350	1441	10367	9280	1661	1999
Testing	646	545	1244	64	1174	284	166	92	523	454	74	103

$$\mathcal{L}_{adv}^l = \mathbb{E}[\mathcal{S}(\mathbf{D}_{real}(\mathbf{G}(I_i, \mathbf{a}))) + \mathcal{S}(-\mathbf{D}_{real}(I_{gt}))] \quad (7)$$

Attribute Construction Loss. We use attribute construction loss \mathcal{L}_{ac} to measure whether the generated samples construct the desired attributes properly according to attribute shifting vector \mathbf{a} . Considering attribute data follows the normal distribution, we use the mean squared error. Our goal is not only to generate the desired attributes but also to control the attributes’ intensities. We train the generator and discriminator to minimize \mathcal{L}_{ac}^r and \mathcal{L}_{ac}^l , respectively.

$$\mathcal{L}_{ac}^r = \mathbb{E}[(\mathbf{D}_c(I_{gt}) - u_i)^2] \quad (8)$$

$$\mathcal{L}_{ac}^l = \mathbb{E}[(\mathbf{G}(I_i, \mathbf{a}) - \mathbf{a} - u_i)^2] \quad (9)$$

For $u_i = 1$ and $u_i = -1$ while using MSE loss, 0 is the boundary for each class. Thus, the actual value of $\mathbf{a} \in [-1, 3]$ if $u_i = 1$, otherwise $\mathbf{a} \in [-3, 1]$.

Image Reconstruction Loss. The generator \mathbf{G} needs to reconstruct image I_{gt} when the attributes shifting vector $\mathbf{a} = \mathbf{0} \in \mathbb{R}^{|\mathbf{A}|}$. Similar to the literature [7, 6, 5, 2, 17], we use L1 loss for this.

$$\mathcal{L}_{rec} = \mathbb{E}\|\|I_{gt} - \mathbf{G}(I_i, \mathbf{0})\| \quad (10)$$

Perceptual Loss. We use the perceptual loss $\mathcal{L}_{percept}$ [9] to improve high-level content similarity between generated images and ground truth images. We use Φ to denote the intermediate feature maps of VGG16 networks [26].

$$\mathcal{L}_{percept} = \mathbb{E}\|\|\sum_{j=1} \Phi(I_{gt}) - \Phi(\mathbf{G}(I_i, \mathbf{0}))\| \quad (11)$$

R1 Regularization. We use R1 regularization [19] to penalize the gradients of ground truth samples and encourage the discriminator to stay in Nash-equilibrium. The key idea is to penalize the gradients for predicting the ground truth images as fake samples.

$$\mathcal{L}_{R1} := \mathbb{E}\|\|\nabla \mathcal{S}(\mathbf{D}_{real}(I_{gt}))\|^2 \quad (12)$$

Final Objectives. The final objective functions for the generator \mathbf{G} and discriminator \mathbf{D} are as follows:

$$\begin{aligned} \mathcal{L}_G = & \lambda_{adv}^r \mathcal{L}_{adv}^r + \lambda_{ac}^r \mathcal{L}_{ac}^r \\ & + \lambda_{rec} \mathcal{L}_{rec} + \lambda_{percept} \mathcal{L}_{percept} \end{aligned} \quad (13)$$

$$\mathcal{L}_D = \lambda_{adv}^l \mathcal{L}_{adv}^l + \lambda_{ac}^l \mathcal{L}_{ac}^l + \lambda_{R1} \mathcal{L}_{R1} \quad (14)$$

Where hyper-parameters, $\lambda_{[\cdot]}$ control the importance of each objective.

4. Experiments

Dataset. We use high-quality face dataset CelebAMask-HQ [15]. For this work, we resize all images to resolution 256×256 and 512×512 . We select every 20th images as the testing fold, and the remaining images are in the training fold. There are 28,000 and 2,000 images for training and testing, respectively. We select twelve state-like attributes, including Smiling, Male, No_Beard, Eyeglasses, Young, Bangs, Narrow_Eyes, Pale_Skin, Big_Lips, Big_Nose, Mustache, and Chubby. The statistic of each attribute in the training and testing fold are summarised in Table 1. To obtain face sketches, we use HED edge detector [29], and post-process with the steps employed by Isola *et al.* [7]. Because of laborious costs and difficulty in collecting various drawings and images pair, we synthesize the real drawing from edge-based sketches [30, 7, 8, 22].

Methods for Comparison. We compare our work with state-of-the-art attribute generation methods, AttGAN [5], and STGAN [17] with their published recommended settings. Although those methods are originally designed to manipulate attributes of photo-realistic images, we apply them to our problem. We present visual results of AttGAN and STGAN with resolution 256×256 , because these models cannot work well in 512×512 resolution [5, 17]. However, our framework works in both 256×256 and 512×512 resolutions. For better visualization in the micro changes of facial attributes, we present our result for resolution 512×512 in the comparison of intensity control (Figure 5). We also compare the final recommendation of our approach with several plausible alternatives. For example, in S2F-BCE, we replace the MSE loss based attribute reconstruction loss with BCE loss. In S2F-CT, we remove Attribute Mapping Networks in *S2FGAN* and concatenate the labels with decoded input. This strategy is similar to previous literature [5, 2, 17, 14], and further helps to investigate

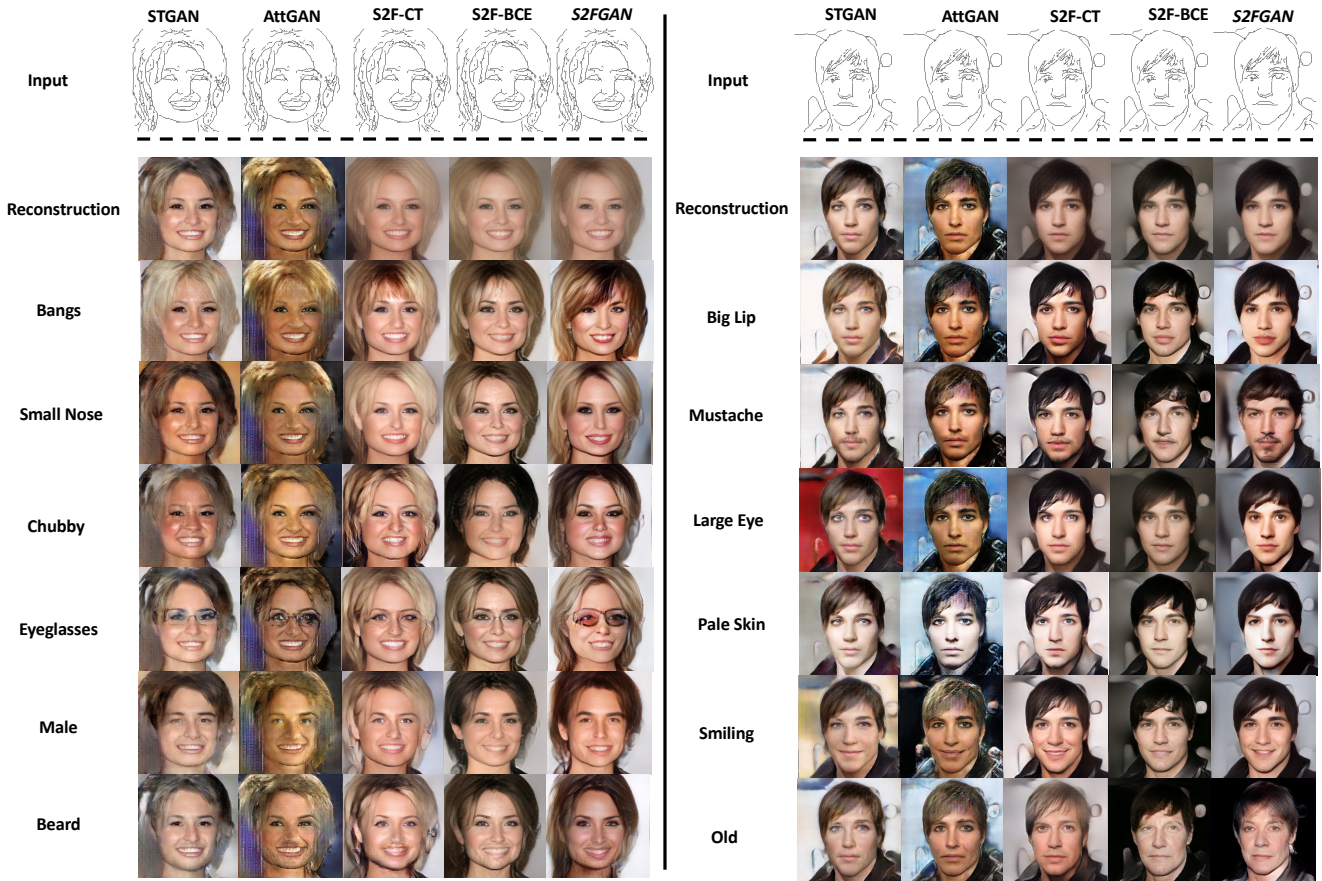


Figure 3: Single attribute editing results for STGAN [17], AttGAN [5], S2F-CT, S2F-BCE and S2FGAN.

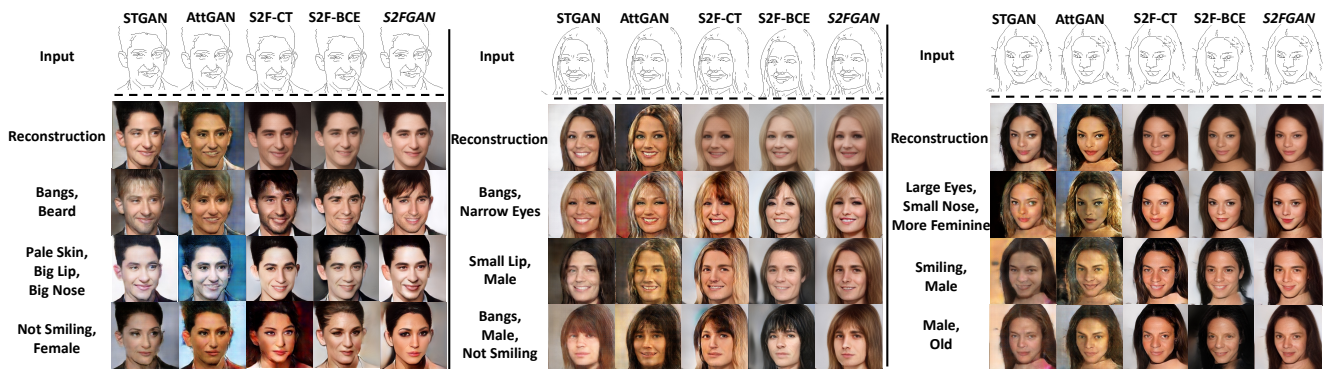


Figure 4: Multi-attribute editing results for AttGAN [5], STGAN [17], S2F-CT, S2F-BCE and S2FGAN.

the effectiveness of Attribute Mapping Networks. Other notable attribute editing works such as [2, 14, 25] do not work when sketches are used as input. As evidence, StarGAN [2] required the cycle loss to train. FaderNetwork [14] relies on the existence of a disentangled latent space that does not contain information about the attributes of interest. InterfaceGAN [25] uses an optimization-based approach to decode the image to latent code that does not work on our problem.

Implementation Details.¹ We train our model for 200 epochs for each stage in progressively training under Adam optimizer with learning rate 0.015. The decays of Adam optimizer are set to 0.5 and 0.999. Our model is trained on four Nvidia Tesla Volta V100-SXM2-32GB with Intel Xeon Cascade Lake Platinum 8268 (2.90GHz) CPUs. We use batch size 64 for training of 512×512 model,

¹Code and models are available at: <https://github.com/Yan98/S2FGAN>

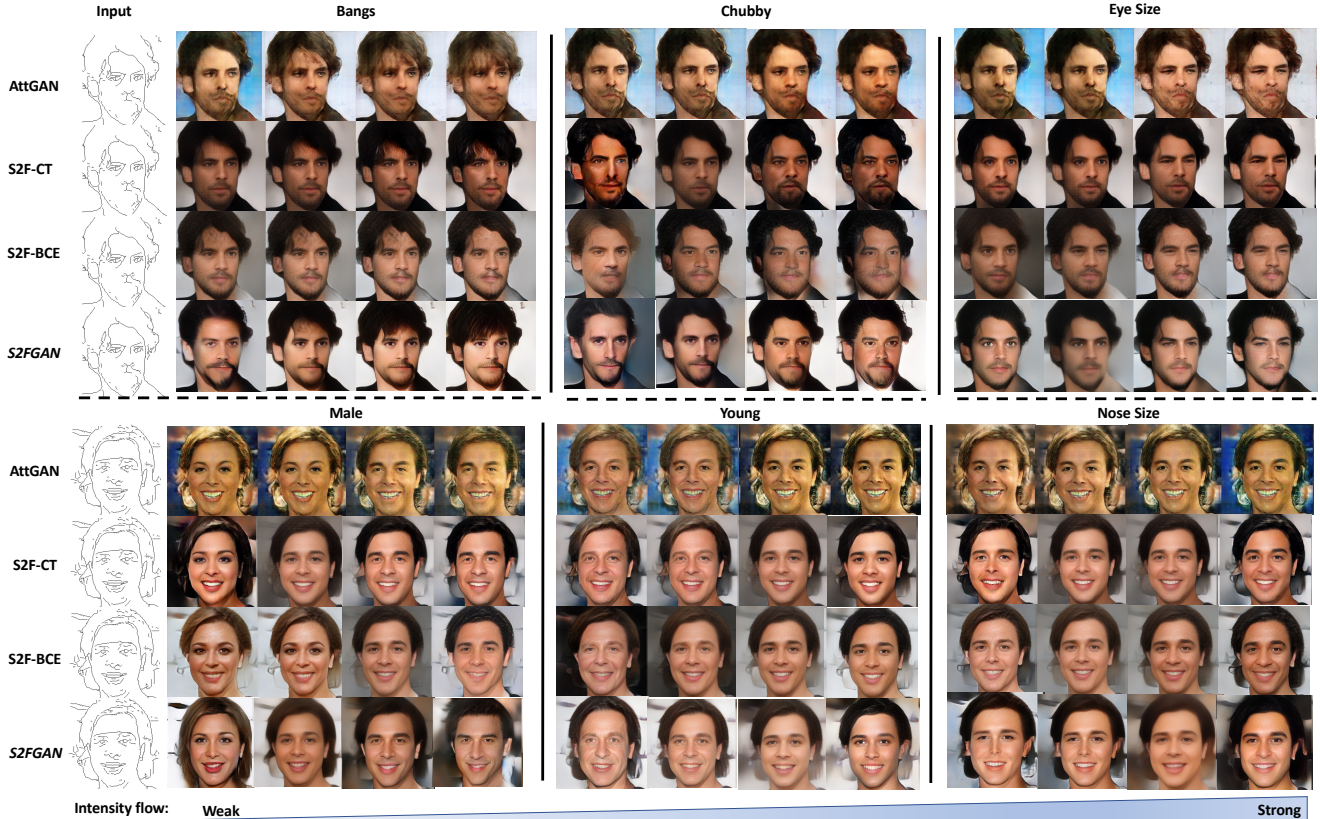


Figure 5: Intensity control for AttGAN [5], S2F-CT, S2F-BCE and S2FGAN.

and batch size 160 for other resolutions. Following StyleGAN [11, 12], all the layers use equalized training trick. Specifically, the trainable parameters are initialized by using the normal distribution, and the weights are explicitly scaled by $\frac{2}{\sqrt{\text{number of parameters}}}$ during forwarding passes for each layer. This improves the stability of training. During training, images and corresponding sketches are randomly cropped and resized with ratio 0.8 and probability 0.5. We randomly used horizontal flip with probability of 0.5 also. For \mathcal{L}_G , we set $\lambda_{adv}^r, \lambda_{ac}^r, \lambda_{rec}$ and $\lambda_{percept}$ to 1, 1, 4 and 3, respectively. For \mathcal{D} , we set $\lambda_{adv}^l, \lambda_{ac}^l$ and λ_{R1} to 1, 1 and 5, respectively. For the perceptual Loss, $\mathcal{L}_{percept}$, we use *ReLU1*, *ReLU2*, *ReLU3* and *ReLU4* of VGG16 [26] (which is pretrained on ImageNet) with weights $\frac{1}{8}, \frac{1}{4}, \frac{1}{2}$ and 1. See the **supplementary material** for detailed network architecture and parameters.

4.1. Sketch-to-Image Translation

Attribute Editing. We present the comparison of S2FGAN and baseline methods for single and multiple attribute editing. For the single attribute case (see Figure 3), AttGAN [5] fails in the majority of attribute editing cases. Also, the label concatenation based methods STGAN [17],

ATTGAN [5], and S2F-CT have weak editing effect, for example for the “Old” case. Note that adding or removing the attributes “Beard” and “Mustache” lead to similar impacts because those two attributes are highly correlated. For multi-attribute editing cases (see Figure 4), apart from AttGAN [5], the rest of the methods reconstruct with the face with similar appearance and color space. [17, 5] sometimes ignores part of the attributes that need to be changed, such as “Pale Skin”, “Big Lip”, and “Big Nose”, “Male” and “Old” editing cases. Moreover, those methods usually fail to retouch the existing attributes such as to change “Nose Size”. In all attribute editing cases, methods can preserve the appearance of faces when they shift the attributes. However, face distortions exist in [5], because this method is originally designed for photo-realistic face input. Here, we consider a more general case that uses attribute editing to aid sketch-to-image translations. Label concatenation based facial attribute editing methods [2, 5, 14, 17] share the same convolutional weights to all inputs. Instead, we scale the weights of the Style Aware Decoder by using the Attribute Mapping Network where different inputs use distinct weights for decoding. Therefore, the S2FGAN and S2F-BCE have better performance in our attribute editing

Table 2: Quantitative evaluation: facial attributes editing accuracy and image quality.

Models	Attribute classification accuracy (%)												FID score
	Smiling	Male	No_Beard	Eyeglasses	Young	Bangs	Narrow_Eyes	Pale_Skin	Big_Lips	Big_Nose	Mustache	Chubby	
AttGAN [5]	39.9	20.2	12.1	60.7	17.2	41.9	78.6	86.5	55.7	39.5	15.6	9.6	70.4
STGAN [17]	89.6	65.4	76.1	97.3	80.9	87.7	94.0	90.5	69.0	71.3	47.3	40.9	42.3
S2FGAN-BCE	90.4	63.1	54.9	91.6	90.2	83.5	97.5	81.4	89.5	93.1	45.3	22.0	39.0
S2FGAN-CT	99.9	88.1	94.1	81.8	83.9	99.4	93.8	88.5	80.3	90.5	48.7	27.1	37.7
<i>S2FGAN</i>	99.7	95.5	97.5	99.9	97.5	99.5	98.8	96.9	89.6	98.5	54.5	71.7	35.1
Ground Truth	93.0	97.6	95.8	99.5	87.9	94.0	91.0	95.7	68.7	80.3	95.9	94.4	-

problem.

Attribute Intensity Control. We compare our proposed architecture with AttGAN [5], S2F-CT, S2F-BCE for attribute intensity control in Figure 5. Our proposed network performs better in controlling the state-like attributes, such as smiling, chubby, young, and so on. One can notice that AttGAN [5] suffers from image distortion heavily. When modifying existing attributes such as lips and nose size, the AttGAN [5] and S2F-CT could not achieve expected performance. These methods control the attribute editing based on concatenation of down-sampled inputs and scaled labels, which lacks centralized coordination for all convolution layers. Thus, the results lack continuity and variation. Our proposed architecture is more adapted to generating photo-realistic images from a sketch with attribute intensity control. We present more qualitative results in the **supplementary material**.

Quantitative Evaluation. In Table 2, we use a classifier suggested by He *et.al* [5] to validate the accuracy of attribute editing for our model. The evaluation classifier is trained on our training data of CelebAMask-HQ dataset [15] for resolution 128×128 . All the models edit attributes in resolution 256×256 . We bilinearly downsample the generated images to resolution 128×128 before feeding into the evaluation classifier. Our proposed framework, *S2FGAN*, achieves the best performance except for the smiling editing task. There is only 0.2% difference between our model and the best performing model in the smiling editing tasks. We also present the performance of the classifier on real testing data in the last row (ground truth) of Table 2. Our model can control attribute intensity, which can construct obvious attributes for the evaluation. It also can enable the evaluation classifier to easily identify the edited attributes. Moreover, we use Frechet Inception Score (FID) to measure diversity and quality of synthesized images. *S2FGAN* achieves the best FID scores, which means our model has the closest distribution to the ground truth image distribution.

4.2. Mask-to-Image Translation

Our approach can generate photo-realistic faces from non-photo-realistic input. In addition to sketches, mask images can be a possible option. Comparing masks with

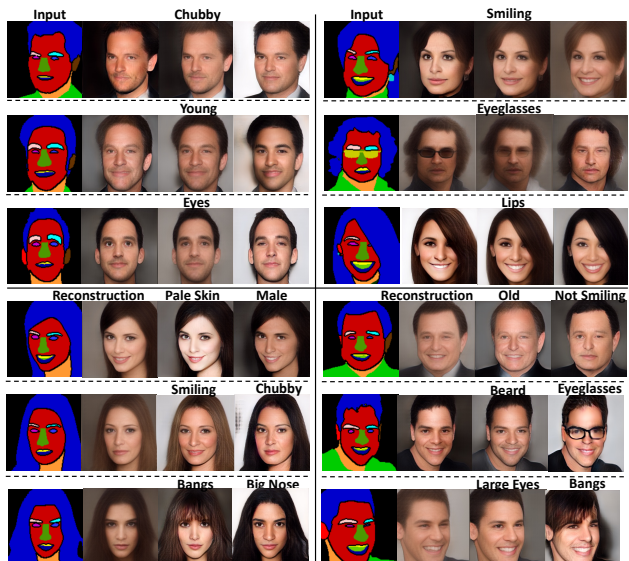


Figure 6: Attribute editing results for mask-to-image translation. Top three rows: intensity control. Bottom three rows: attribute editing.

sketches, the mask is weaker in expressing abstract attributes and provides more regular views of objects. Here, we explore attribute editing for the mask to image translation. The results are shown in Figure 6. We replace the sketch with masks from CelebAMASK-HQ data [15], and adopts the settings described in Section 4. The *S2FGAN* still achieves remarkable performance in this task and deserves attention for aiding mask-to-image translation problems.

5. Conclusion

This paper proposes a photo-realistic face generation model, *S2FGAN*, given a sketch image as input. It can ascribe attributes on the generated face and include smooth manipulation over intensities of attributes. Further, our generated face preserves subject identity considering both single and multi-attribute editing cases. By separating the appearance latent space and attribute latent space, we can shift face attributes that are conditional on a given sketch. Experiments on large face collection datasets demonstrate that *S2FGAN* can accurately edit face attributes with more ex-

cellent controllability, even with non-photo-realistic inputs.

References

- [1] Piotr Bojanowski, Armand Joulin, David Lopez-Paz, and Arthur Szlam. Optimizing the latent space of generative networks. In Jennifer G. Dy and Andreas Krause, editors, *Proceedings of the 35th International Conference on Machine Learning, ICML 2018, Stockholmsmässan, Stockholm, Sweden, July 10-15, 2018*, volume 80 of *Proceedings of Machine Learning Research*, pages 599–608. PMLR, 2018. [2](#)
- [2] Yunjey Choi, Min-Je Choi, Munyoung Kim, Jung-Woo Ha, Sunghun Kim, and Jaegul Choo. Stargan: Unified generative adversarial networks for multi-domain image-to-image translation. *CoRR*, abs/1711.09020, 2017. [1](#), [2](#), [4](#), [5](#), [6](#), [7](#)
- [3] Tali Dekel, Chuang Gan, Dilip Krishnan, Ce Liu, and William T. Freeman. Sparse, smart contours to represent and edit images. In *2018 IEEE Conference on Computer Vision and Pattern Recognition, CVPR 2018, Salt Lake City, UT, USA, June 18-22, 2018*, pages 3511–3520. IEEE Computer Society, 2018. [3](#)
- [4] Ian J. Goodfellow, Jean Pouget-Abadie, Mehdi Mirza, Bing Xu, David Warde-Farley, Sherjil Ozair, Aaron C. Courville, and Yoshua Bengio. Generative adversarial nets. In Zoubin Ghahramani, Max Welling, Corinna Cortes, Neil D. Lawrence, and Kilian Q. Weinberger, editors, *Advances in Neural Information Processing Systems 27: Annual Conference on Neural Information Processing Systems 2014, December 8-13 2014, Montreal, Quebec, Canada*, pages 2672–2680, 2014. [1](#), [4](#)
- [5] Zhenliang He, Wangmeng Zuo, Meina Kan, Shiguang Shan, and Xilin Chen. AttnGAN: Facial attribute editing by only changing what you want. *IEEE Trans. Image Process.*, 28(11):5464–5478, 2019. [1](#), [2](#), [3](#), [4](#), [5](#), [6](#), [7](#), [8](#), [11](#)
- [6] Xun Huang, Ming-Yu Liu, Serge J. Belongie, and Jan Kautz. Multimodal unsupervised image-to-image translation. In Vittorio Ferrari, Martial Hebert, Cristian Sminchisescu, and Yair Weiss, editors, *Computer Vision - ECCV 2018 - 15th European Conference, Munich, Germany, September 8-14, 2018, Proceedings, Part III*, volume 11207 of *Lecture Notes in Computer Science*, pages 179–196. Springer, 2018. [2](#), [5](#)
- [7] Phillip Isola, Jun-Yan Zhu, Tinghui Zhou, and Alexei A. Efros. Image-to-image translation with conditional adversarial networks. *CoRR*, abs/1611.07004, 2016. [1](#), [2](#), [3](#), [4](#), [5](#), [11](#)
- [8] Youngjoo Jo and Jongyoul Park. SC-FEGAN: face editing generative adversarial network with user’s sketch and color. *CoRR*, abs/1902.06838, 2019. [2](#), [4](#), [5](#)
- [9] Justin Johnson, Alexandre Alahi, and Li Fei-Fei. Perceptual losses for real-time style transfer and super-resolution. In Bastian Leibe, Jiri Matas, Nicu Sebe, and Max Welling, editors, *Computer Vision - ECCV 2016 - 14th European Conference, Amsterdam, The Netherlands, October 11-14, 2016, Proceedings, Part II*, volume 9906 of *Lecture Notes in Computer Science*, pages 694–711. Springer, 2016. [5](#)
- [10] Tero Karras, Timo Aila, Samuli Laine, and Jaakko Lehtinen. Progressive growing of gans for improved quality, stability, and variation. In *6th International Conference on Learning Representations, ICLR 2018, Vancouver, BC, Canada, April 30 - May 3, 2018, Conference Track Proceedings*. OpenReview.net, 2018. [2](#), [3](#)
- [11] Tero Karras, Samuli Laine, and Timo Aila. A style-based generator architecture for generative adversarial networks. In *IEEE Conference on Computer Vision and Pattern Recognition, CVPR 2019, Long Beach, CA, USA, June 16-20, 2019*, pages 4401–4410. Computer Vision Foundation / IEEE, 2019. [2](#), [3](#), [4](#), [7](#)
- [12] Tero Karras, Samuli Laine, Miika Aittala, Janne Hellsten, Jaakko Lehtinen, and Timo Aila. Analyzing and improving the image quality of stylegan. In *2020 IEEE/CVF Conference on Computer Vision and Pattern Recognition, CVPR 2020, Seattle, WA, USA, June 13-19, 2020*, pages 8107–8116. IEEE, 2020. [2](#), [4](#), [7](#), [11](#)
- [13] Samuli Laine. Feature-based metrics for exploring the latent space of generative models. In *6th International Conference on Learning Representations, ICLR 2018, Vancouver, BC, Canada, April 30 - May 3, 2018, Workshop Track Proceedings*. OpenReview.net, 2018. [2](#)
- [14] Guillaume Lample, Neil Zeghidour, Nicolas Usunier, Antoine Bordes, Ludovic Denoyer, and Marc’Aurelio Ran-zato. Fader networks: Manipulating images by sliding attributes. In Isabelle Guyon, Ulrike von Luxburg, Samy Bengio, Hanna M. Wallach, Rob Fergus, S. V. N. Vishwanathan, and Roman Garnett, editors, *Advances in Neural Information Processing Systems 30: Annual Conference on Neural Information Processing Systems 2017, 4-9 December 2017, Long Beach, CA, USA*, pages 5967–5976, 2017. [1](#), [2](#), [4](#), [5](#), [6](#), [7](#)
- [15] Cheng-Han Lee, Ziwei Liu, Lingyun Wu, and Ping Luo. MaskGAN: Towards diverse and interactive facial image manipulation. In *2020 IEEE/CVF Conference on Computer Vision and Pattern Recognition, CVPR 2020, Seattle, WA, USA, June 13-19, 2020*, pages 5548–5557. IEEE, 2020. [5](#), [8](#)
- [16] Ming-Yu Liu, Thomas Breuel, and Jan Kautz. Unsupervised image-to-image translation networks. In Isabelle Guyon, Ulrike von Luxburg, Samy Bengio, Hanna M. Wallach, Rob Fergus, S. V. N. Vishwanathan, and Roman Garnett, editors, *Advances in Neural Information Processing Systems 30: Annual Conference on Neural Information Processing Systems 2017, 4-9 December 2017, Long Beach, CA, USA*, pages 700–708, 2017. [2](#)
- [17] Ming Liu, Yukang Ding, Min Xia, Xiao Liu, Errui Ding, Wangmeng Zuo, and Shilei Wen. STGAN: A unified selective transfer network for arbitrary image attribute editing. In *IEEE Conference on Computer Vision and Pattern Recognition, CVPR 2019, Long Beach, CA, USA, June 16-20, 2019*, pages 3673–3682. Computer Vision Foundation / IEEE, 2019. [1](#), [2](#), [4](#), [5](#), [6](#), [7](#), [8](#), [11](#)
- [18] Yongyi Lu, Shangzhe Wu, Yu-Wing Tai, and Chi-Keung Tang. Image generation from sketch constraint using contextual GAN. In Vittorio Ferrari, Martial Hebert, Cristian Sminchisescu, and Yair Weiss, editors, *Computer Vision - ECCV 2018 - 15th European Conference, Munich, Germany, September 8-14, 2018, Proceedings, Part XVI*, volume 11220 of *Lecture Notes in Computer Science*, pages 213–228. Springer, 2018. [1](#), [2](#), [3](#)

- [19] Lars M. Mescheder, Andreas Geiger, and Sebastian Nowozin. Which training methods for gans do actually converge? In Jennifer G. Dy and Andreas Krause, editors, *Proceedings of the 35th International Conference on Machine Learning, ICML 2018, Stockholmsmässan, Stockholm, Sweden, July 10-15, 2018*, volume 80 of *Proceedings of Machine Learning Research*, pages 3478–3487. PMLR, 2018. 5
- [20] Mehdi Mirza and Simon Osindero. Conditional generative adversarial nets. *CoRR*, abs/1411.1784, 2014. 1, 2
- [21] Stanislav Pidhorskyi, Donald A. Adjeroh, and Gianfranco Doretto. Adversarial latent autoencoders. In *2020 IEEE/CVF Conference on Computer Vision and Pattern Recognition, CVPR 2020, Seattle, WA, USA, June 13-19, 2020*, pages 14092–14101. IEEE, 2020. 2
- [22] Tiziano Portenier, Qiyang Hu, Attila Szabó, Siavash Arjomand Bigdeli, Paolo Favaro, and Matthias Zwicker. Faceshop: deep sketch-based face image editing. *ACM Trans. Graph.*, 37(4):99:1–99:13, 2018. 2, 5
- [23] Olaf Ronneberger, Philipp Fischer, and Thomas Brox. U-net: Convolutional networks for biomedical image segmentation. In Nassir Navab, Joachim Hornegger, William M. Wells III, and Alejandro F. Frangi, editors, *Medical Image Computing and Computer-Assisted Intervention - MICCAI 2015 - 18th International Conference Munich, Germany, October 5 - 9, 2015, Proceedings, Part III*, volume 9351 of *Lecture Notes in Computer Science*, pages 234–241. Springer, 2015. 4, 11
- [24] Hang Shao, Abhishek Kumar, and P. Thomas Fletcher. The riemannian geometry of deep generative models. In *2018 IEEE Conference on Computer Vision and Pattern Recognition Workshops, CVPR Workshops 2018, Salt Lake City, UT, USA, June 18-22, 2018*, pages 315–323. IEEE Computer Society, 2018. 2
- [25] Yujun Shen, Jinjin Gu, Xiaoou Tang, and Bolei Zhou. Interpreting the latent space of gans for semantic face editing. In *2020 IEEE/CVF Conference on Computer Vision and Pattern Recognition, CVPR 2020, Seattle, WA, USA, June 13-19, 2020*, pages 9240–9249. IEEE, 2020. 1, 2, 3, 4, 6
- [26] Karen Simonyan and Andrew Zisserman. Very deep convolutional networks for large-scale image recognition. In Yoshua Bengio and Yann LeCun, editors, *3rd International Conference on Learning Representations, ICLR 2015, San Diego, CA, USA, May 7-9, 2015, Conference Track Proceedings*, 2015. 5, 7
- [27] Paul Upchurch, Jacob R. Gardner, Geoff Pleiss, Robert Pless, Noah Snavely, Kavita Bala, and Kilian Q. Weinberger. Deep feature interpolation for image content changes. In *2017 IEEE Conference on Computer Vision and Pattern Recognition, CVPR 2017, Honolulu, HI, USA, July 21-26, 2017*, pages 6090–6099. IEEE Computer Society, 2017. 2
- [28] Ting-Chun Wang, Ming-Yu Liu, Jun-Yan Zhu, Andrew Tao, Jan Kautz, and Bryan Catanzaro. High-resolution image synthesis and semantic manipulation with conditional gans. In *2018 IEEE Conference on Computer Vision and Pattern Recognition, CVPR 2018, Salt Lake City, UT, USA, June 18-22, 2018*, pages 8798–8807. IEEE Computer Society, 2018. 1, 2, 3
- [29] Saining Xie and Zhuowen Tu. Holistically-nested edge detection. In *2015 IEEE International Conference on Computer Vision, ICCV 2015, Santiago, Chile, December 7-13, 2015*, pages 1395–1403. IEEE Computer Society, 2015. 5
- [30] Shuai Yang, Zhangyang Wang, Jiaying Liu, and Zongming Guo. Deep plastic surgery: Robust and controllable image editing with human-drawn sketches. *CoRR*, abs/2001.02890, 2020. 1, 2, 3, 5

6. Additional Implementation details

Our *S2FGAN* has two key components: a Generator (Appearance Latent Encoder, Attribute Mapping Network, and Style Aware Decoder) and a Discriminator. Here we provide the details.

Notions. In Figure 9, Figure 8, and Figure 7, we use the abbreviations. C stands for the convolution 2d layer. CT stands for the transposed convolution 2d layer. CO stands for the convolution 1d layer. S stands for the stride parameter. P stands for the padding parameter. The number following the layer name denotes the output of the layer. LReLU stands for LeakyReLU, where we always use slope 0.2. IN stands for instance normalization. The parameter for the UpSample layer is the scale factor, where we always use the nearest Upsample layer. Blur stands for Blur layer, we use the same blur kernel $[1, 3, 3, 1]$ as the StyleGAN [12], and the padding is always set to 1.

Generator. Our generator has U-Net-like [23] skip connections. We use the Style Block from StyleGAN [12] as the backbone of our Style Aware Decoder. The generator architecture is illustrated in Figure 9.

Attribute Mapping Networks. The Attribute Mapping Network takes the final output r_i of the Appearance Latent Encoder and the attribute shifting vector a as inputs, and produces output vector d_i as shown in Figure 8. We use the d_i to scale the convolution weights of the Style Aware Decoder.

Discriminator. We adapt PatchGAN [7] to our discriminator. Our discriminator outputs the probabilities of the input belonging to the photo-realistic domain and the attribute class domains. The architecture is shown in Figure 7.

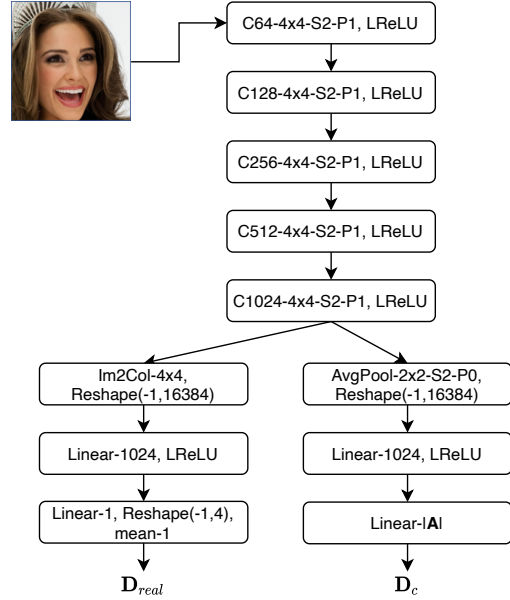


Figure 7: The discriminator structure of *S2FGAN*

7. Additional Qualitative Results

We provide the additional comparison with AttGAN [5], STGAN[17], S2F-BCE, and S2F-CT in Figure 10, Figure 11 and Figure 12. We also provide 512×512 resolution samples of our *S2FGAN* in Figure 13 and Figure 14.

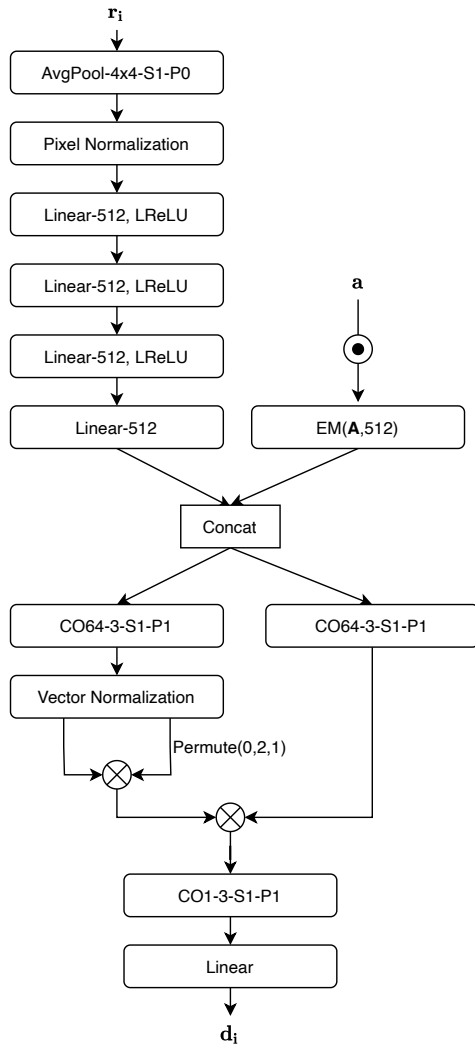


Figure 8: The Attribute Mapping Network of *S2FGAN*

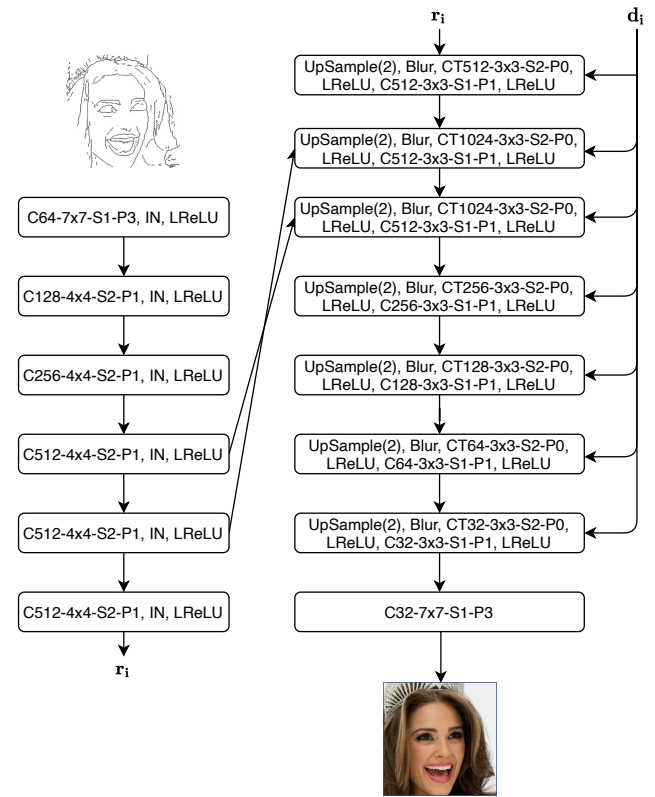


Figure 9: The Appearance Latent Encoder and Style Aware Decoder of *S2FGAN*

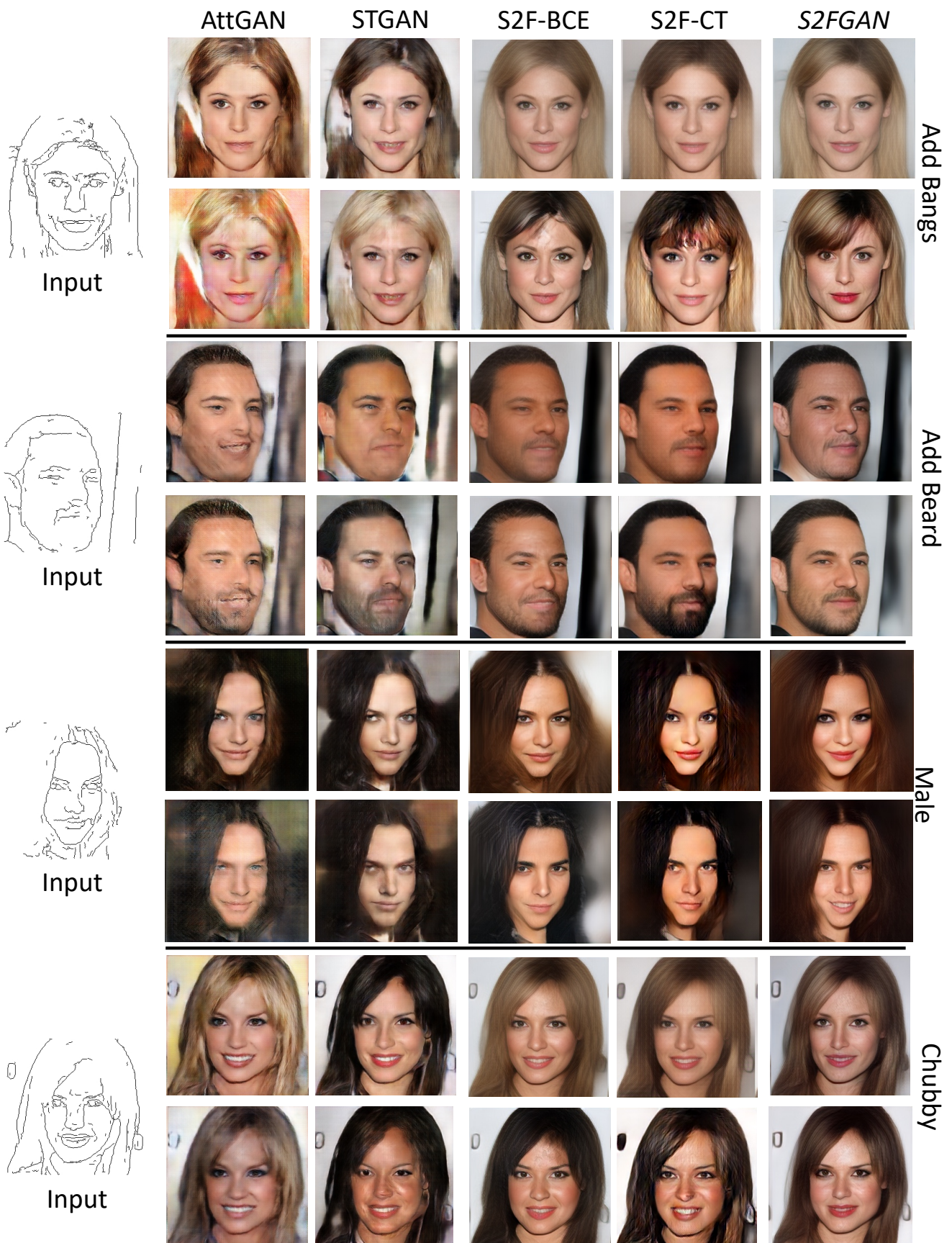


Figure 10: Visual comparison results with 256×256 resolution. Every first and second row shows the reconstructed and attributes manipulated faces, respectively. The S2FGAN outperforms other methods in image reconstruction and attribute manipulation task.

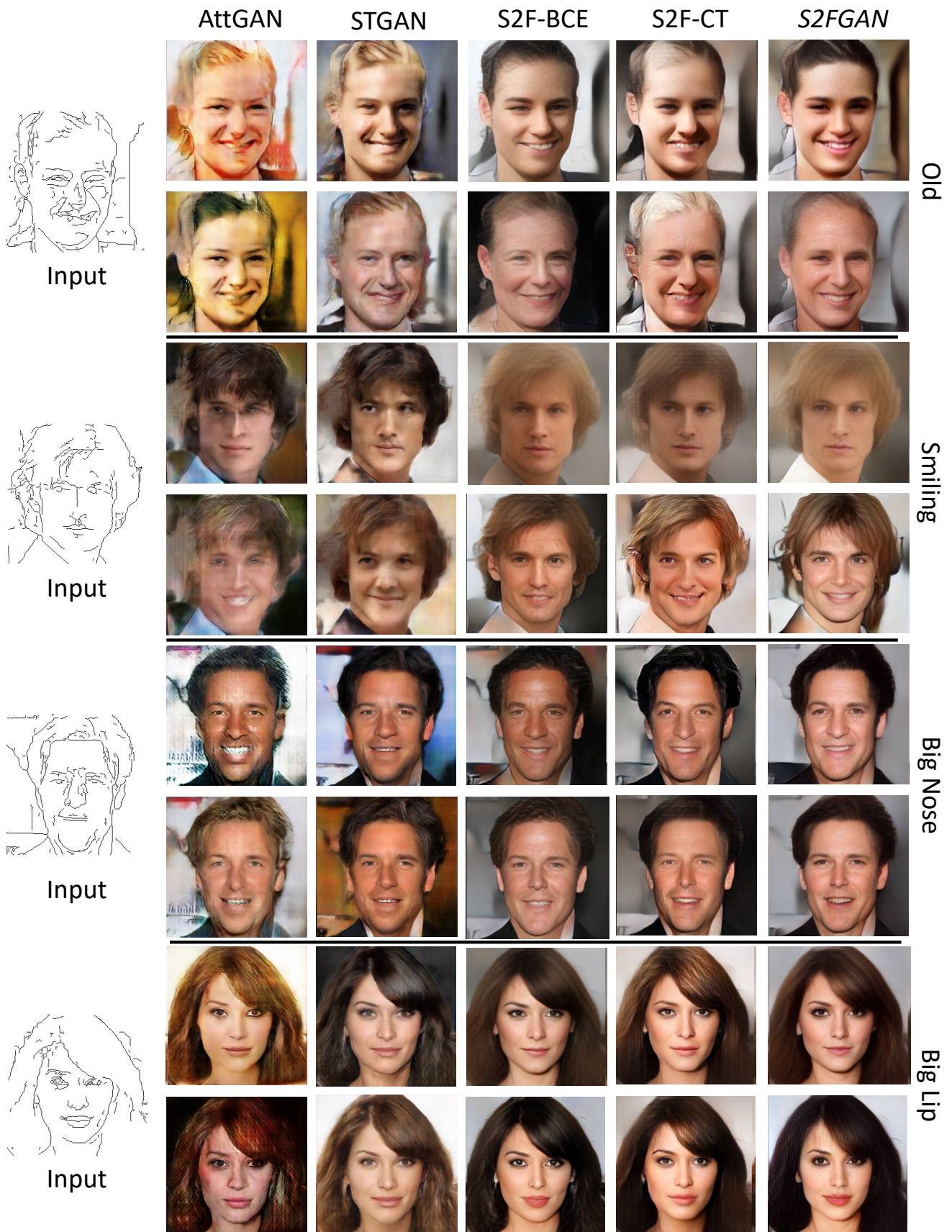


Figure 11: Visual comparison results with 256×256 resolution. Every first and second row shows the reconstructed and attributes manipulated faces, respectively. The *S2FGAN* outperforms other methods in image reconstruction and attribute manipulation task.

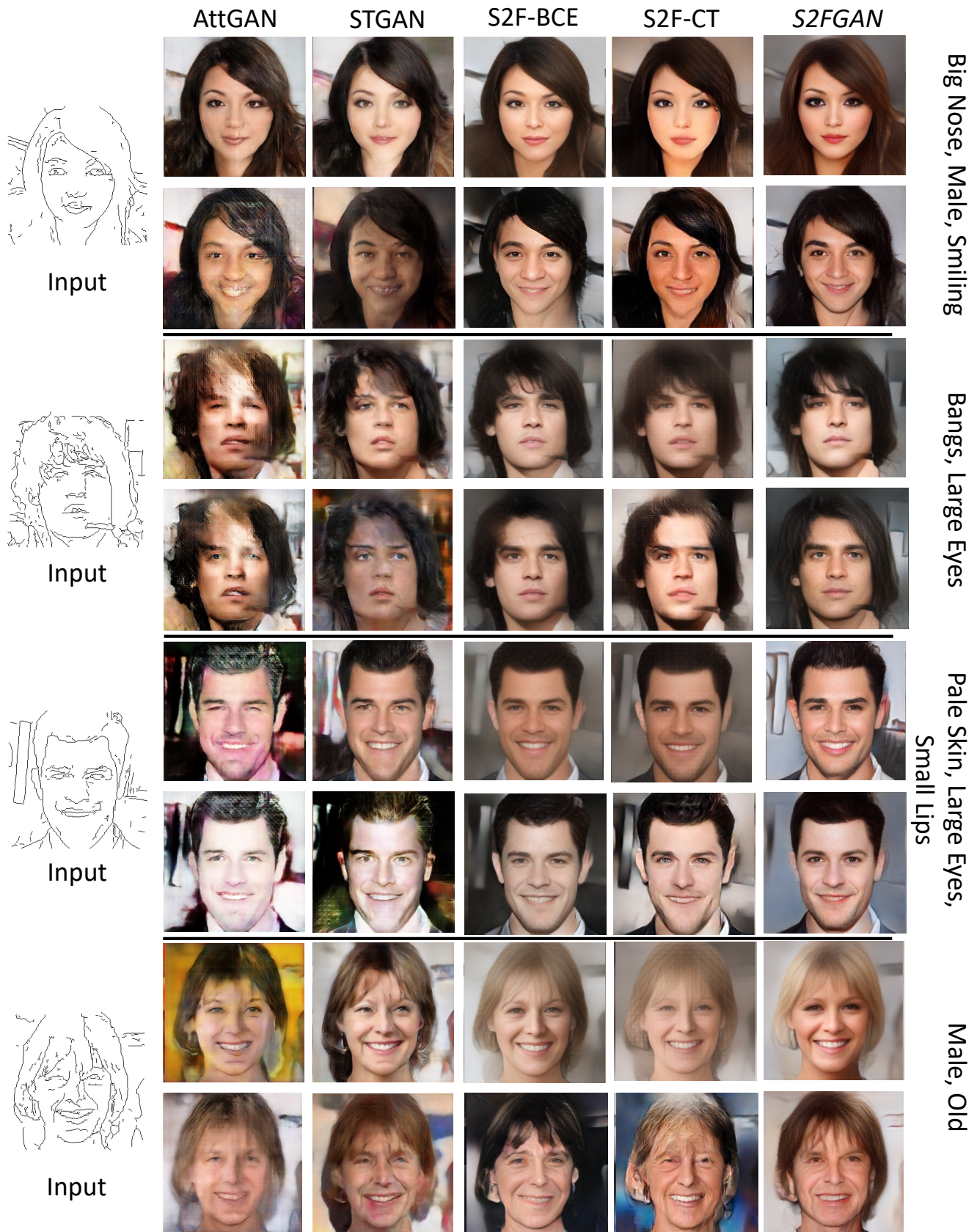


Figure 12: Visual comparison results with 256×256 resolution. Every first and second row shows the reconstructed and attributes manipulated faces, respectively. The *S2FGAN* outperforms other methods in image reconstruction and attribute manipulation task.

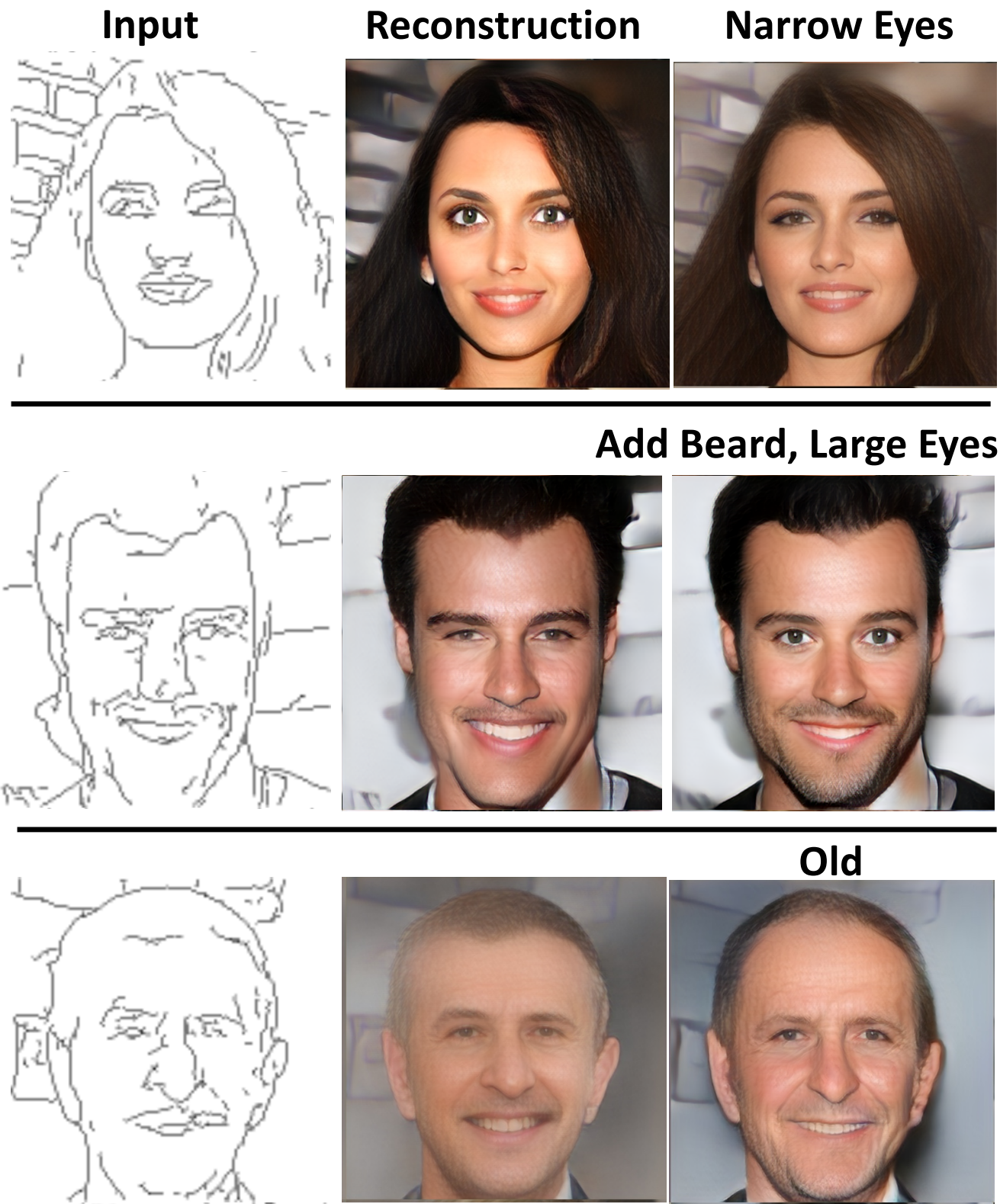
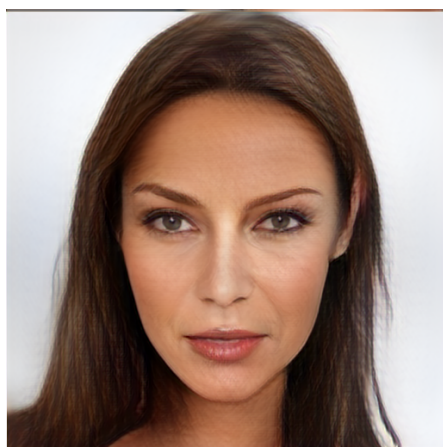


Figure 13: Visual result of *S2FGAN* with 512×512 resolution.

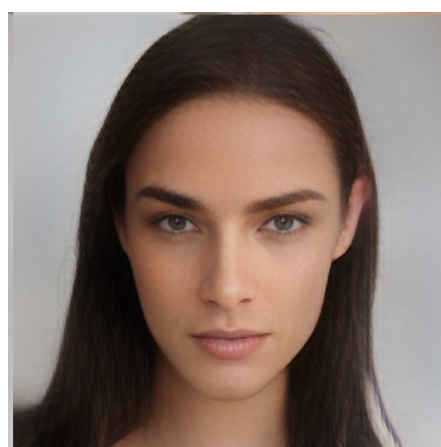
Input



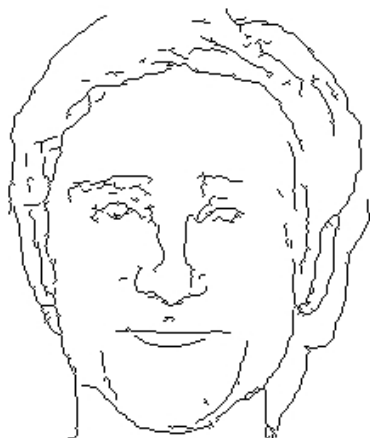
Reconstruction



Young, Male



Pale Skin



Chubby

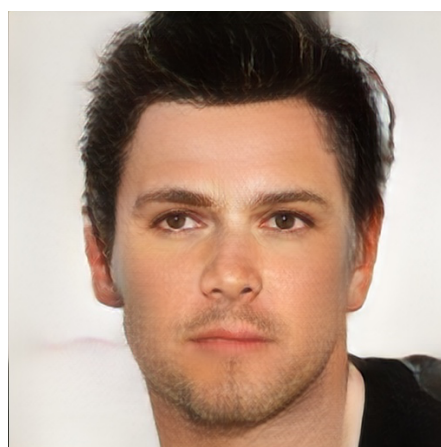
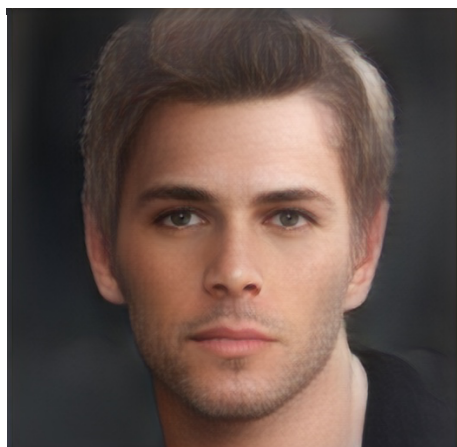
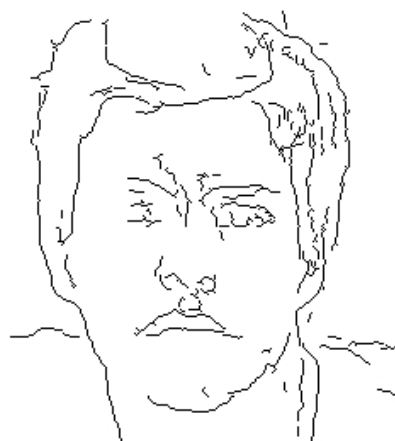


Figure 14: Visual result of *S2FGAN* in 512×512 resolution.